

# A Density Functional Study of a New Family of Anticancer Drugs: Paclitaxel, Taxotere, Epothilone, and Discodermolide

**P. Ballone\***

*Institut für Festkörperforschung, Forschungszentrum Jülich, D-52425 Jülich, Germany, and Max-Planck Institut für Festkörperforschung, Heisenbergstrasse 1, 70569 Stuttgart, Germany*

**M. Marchi**

*Centre Européen de Calcul Atomique et Moléculaire (CECAM), Ecole Normale Supérieure de Lyon, 46 Allée d'Italie, 69364 Lyon, France, and Section de Biophysique des Protéines et des Membranes, DBCM, DSV, CEA, Centre d'Études, Saclay, 91191 Gif-sur-Yvette Cedex, France*

*Received: September 11, 1998; In Final Form: December 28, 1998*

We present a density-functional study of the paclitaxel, taxotere, baccatin III, epothilone-A, and discodermolide molecules in their gas phase. For each of these compounds we determine the geometry and the electronic structure of the ground state and of some isomers and analogues. We find that the central part of all these molecules is insensitive to changes in structure, orientation, and isomerization of its tail and is characterized by a rather large dipole that has similar orientation with respect to the molecular frame. These similarities extend also to the electronic structure. Our results provide an extended and consistent set of data to gauge classical force fields in view of the atomistic investigations of the interaction of these molecules with tubulin.

## 1. Introduction

Paclitaxel and closely related compounds are among the most promising new anticancer drugs. Extensive *in vitro* and *in vivo* experimentation has shown that these molecules prevent the proliferation of cancer cells by promoting the polymerization of tubulin, thus disrupting the mitotic process.<sup>1</sup> Although an atomistic structure of tubulin has recently been proposed,<sup>2</sup> no detailed information is yet available on the microscopic mechanism underlying the activity of these drugs, and the development of improved variants can be carried out only by trial and error.

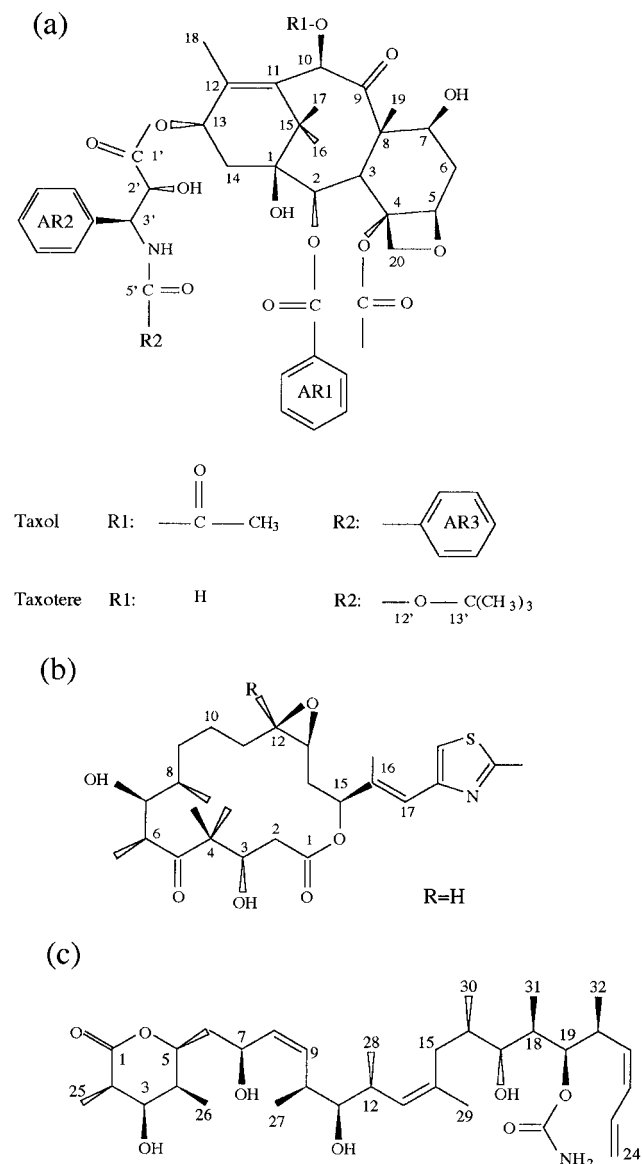
Scheme 1 illustrates the structure of the molecules we investigate. Paclitaxel, taxotere, and baccatin share the same central taxane ring, and differ mainly in the residue attached to the C13 carbon. In the inactive baccatin compound, the residue is a single hydrogen. In paclitaxel and taxotere, both active anticancer drugs, the residue is an elongated, hydrophobic tail. The same central body–tail structure is apparent in epothilone, for which the body is made by a 16-membered macrocyclic lactone ring, and the tail includes a thiazole ring. At first sight, discodermolides have a very different structure, being made of two chains (a long one extends from C1 to C18, and a short one carries a carbamate carbonyl group) joined at the C18–C19 single bond. A closer look at the three-dimensional structure provided by experiments,<sup>3</sup> however, shows that the folded long chain mimics the globular part of the previous molecules, while the short chain might be the analogue of the paclitaxel, taxotere and epothilone tails (see Figure 1). Experimental structure/activity relation studies have focused on the tails of these molecules, which have been shown to be necessary components of the active species.<sup>4,5</sup> However, the central body is also likely to play an important (and yet undiscovered) role, since subtle changes in its structure often produce significant variations in the anticancer activity of these compounds.

In this paper, we have performed a detailed density functional (DFT) study of paclitaxel, baccatin III, taxotere, epothilone-A, and discodermolide. Since our “first principle” investigation is capable of providing unambiguous and parameter-free results, it has considerable advantages with respect to semiempirical or purely classical molecular mechanics approaches. Although still computationally heavy, our DFT calculations on molecules of such large sizes have been made possible by recent advances in the Car–Parrinello technique.<sup>6</sup>

Our main goal in this study has been to single out common features among the drug molecules both at the structural and at the chemical reactivity level. Thus, we have investigated the effect of conformational changes and of isomerization on the optimized structures and characterized the molecular reactivity by the computation of the Fukui orbital. Moreover, we have computed a variety of other properties (like the molecular dipole moments, the atomic electrostatic charges, and the vibrational spectra) in order to provide additional data to parametrize classical force fields for these molecules.

## 2. Computational Method

Our computations are based on the density functional theory (DFT<sup>7</sup>) in the local density plus gradient corrections approximation (LDA+GC<sup>8</sup>). Only valence electrons are included explicitly in the computation, and their interaction with the ionic cores is described by *ab initio* norm-conserving pseudopotentials.<sup>9</sup> Single-electron orbitals are expanded on a basis of plane waves with a kinetic energy cutoff of 70 Ry.<sup>10</sup> Convergence tests show that this cutoff provides interatomic distances which are less than 0.02 Å from the convergence limit. The atomic coordinates are relaxed by the DFT–molecular dynamics method of Car and Parrinello.<sup>6</sup> Optimization is terminated when the forces on the atoms are smaller than  $5 \times 10^{-4}$  hartree atomic units. Because of the complexity of the molecules, and the large

**SCHEME 1: Schematic Structure of (a) the Taxoids, (b) Epithilone, and (c) Discodermolide<sup>a</sup>**


<sup>a</sup> Baccatin III has the same structure of paclitaxel, with the residue at the C13 position replaced by a single hydrogen.

number of nearly equivalent isomers, we have not attempted to identify the global minimum of the energy with respect to all the atomic coordinates, but we have focused on a small number of minima with geometries close to those provided by X-ray diffraction and NMR studies of crystallized samples.<sup>3</sup>

The electronic structure of each molecule at the optimized geometry is analyzed by projecting the Kohn–Sham orbitals on a minimal basis of (pseudo) atomic orbitals.

Vibrational modes are computed by diagonalizing a finite difference approximation for the dynamical matrix.

### 3. Structural Results

The first part of the computation is devoted to the determination of the ground state geometry for the free molecules, whose results are summarized in Tables 1–3. The full list of the optimized atomic positions is available as Supporting Information. Starting from the experimental structures, the DFT optimization produces small<sup>11</sup> but sometimes significant changes, due to (i) structural differences between the crystal and the gas

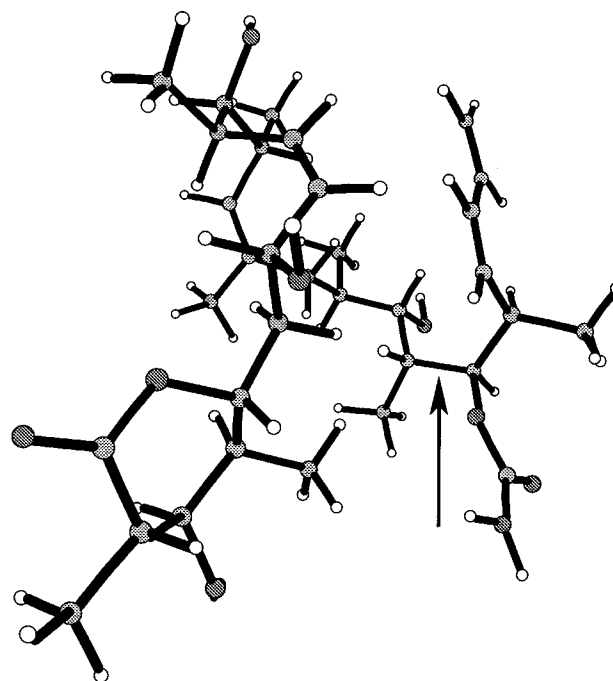


**Figure 1.** Equilibrium structure of the gas-phase discodermolide molecule. The C18–C19 bond is identified by the vertical arrow.

phase, (ii) inaccuracies in the hydrogen positions provided by the X-ray measurements, and (iii) the combined inaccuracies of both the experimental and computational results for the position of the “heavier” atoms. This last problem is the least important, leading to uncertainties of  $\sim 1\%$  in the interatomic distances. By far the largest discrepancies are associated with the H atoms, whose positions cannot be determined accurately by X-ray diffraction.

The structural refinement offered by the computation highlights several features that are important to understand the stability and binding properties of these molecules. In paclitaxel, for instance, we observe the formation of three intramolecular hydrogen bonds,<sup>12</sup> which are not present, or hardly recognizable in the experimental structure. Together with the presence of three hydrophobic phenyl rings, these intramolecular hydrogen bonds help to explain the low solubility of paclitaxel in water. Similar features are observed in taxotere and baccatin III, with, however, some quantitative differences: the number of intramolecular hydrogen bonds is lower than in paclitaxel, and the role of phenyl is obviously reduced.

Visual inspection of the paclitaxel and taxotere structures suggests that large amplitude rotations of the AR2–R2 tail are possible around the C2'–C3' single bond. Our calculation shows that, upon rotating the tail around this bond, the energy increase is always less than 10 kcal/mol, provided that the structure is briefly relaxed by molecular dynamics while keeping constant the C1'–C2'–C3'–N torsional angle. We also found that both paclitaxel and taxotere have low-energy ( $\Delta E \leq 5$  kcal/mol) isomers characterized by a significantly different tail orientation. In these isomers, the rotation of the tail is accompanied by the rearrangement of the intramolecular hydrogen bonds, and by the reorientation of the phenyl groups. Since these complex relaxations provide information about the relative importance of different intramolecular interactions, and enlarge the database for semiempirical modeling, we have included the geometry of these additional isomers in the Supporting Information.

Not unexpectedly, our computation shows that the taxane part of these molecules is insensitive to the composition and

**TABLE 1: Selected Interatomic Distances (Å) and Angles (deg) in Taxol, Taxotere, and Baccatin III<sup>a</sup>**

atoms	taxol	taxotere	baccatin III
C1–C2	1.582	1.574	1.580
C2–C3	1.575	1.580	1.575
C3–C4	1.563	1.559	1.560
C4–C5	1.561	1.557	1.559
C5–C6	1.523	1.518	1.522
C6–C7	1.531	1.530	1.531
C7–C8	1.586	1.600	1.588
C3–C8	1.590	1.590	1.588
C8–C9	1.571	1.547	1.569
C9–O	1.221	1.240	1.222
C9–C10	1.546	1.545	1.549
C10–C11	1.498	1.498	1.503
C11–C12	1.356	1.353	1.356
C12–C13	1.515	1.515	1.525
C13–C14	1.538	1.538	1.542
C14–C1	1.553	1.566	1.549
C1–C15	1.571	1.573	1.570
C11–C15	1.538	1.534	1.539
C4–C20	1.541	1.541	1.540
C20–O	1.465	1.465	1.464
C5–O	1.480	1.479	1.480
C13–O	1.493	1.491	1.459
C1'–O	1.349	1.348	
C1'–C2'	1.532	1.532	
C2'–C3'	1.558	1.551	
C3'–N	1.463	1.454	
C5'–N	1.379	1.370	
C5'–O	1.237	1.232	
C1–C2–C3	119.4	118.2	119.5
C2–C3–C4	111.8	110.7	111.3
C3–C4–C5	119.8	119.6	119.7
C4–C5–C6	120.2	120.5	120.3
C5–C6–C7	113.7	115.4	113.9
C6–C7–C8	112.7	113.3	112.8
C2–C3–C8	115.6	116.0	115.9
C7–C8–C9	102.0	100.4	102.2
C8–C9–C10	120.8	124.5	120.8
C9–C10–C11	114.6	115.3	114.4
C10–C11–C12	120.6	120.7	120.6
C10–C11–C15	119.2	119.0	119.6
C11–C15–C1	105.7	105.6	105.8
C12–C13–C14	113.1	111.7	112.7
C13–C14–C1	116.0	115.4	117.5
C13–CO–C1'	116.4	115.6	
C1'–C2'–C3'	110.4	113.9	
C2'–C3'–N	106.9	109.1	
C3'–N–C5'	120.7	122.4	
C20–O–C5	91.0	91.0	90.9
C4–C20–O	92.2	92.0	92.1

<sup>a</sup> Atom numbers are defined in Scheme 1.

orientation of the tail, underlying the rigidity of the central body. This rigidity is probably in relation to the significant distortion in the taxane rings. Indeed, the matching of rather dissimilar four-, six-, and eight-member rings results in a large stress of the carbon backbone, reflected in deviations of the ideal C–C–C angles as large as 10°, and in smaller but still significant variations in the bonding distances. In addition, the tail geometry appears from our calculation to be insensitive to its orientation with respect to the main molecular body.

By relaxing a few isomers and analogues (similar to those experimentally investigated in ref 4), we have found that the structure of the taxane ring is somewhat more sensitive to the composition and structure of the R1 residue, although, even in this case, the variations are smaller than 0.025 Å and 3° for interatomic distances and angles, respectively.

We emphasize here that the isomers investigated, corresponding to the forms of paclitaxel and taxotere most important for pharmacology, are not energetically the most stable ones, at

**TABLE 2: Selected Interatomic Distances (Å) and Angles (deg) in Epothilone-A and Epothilone-B(2)<sup>a</sup>**

atoms	epothilone-A	epothilone-B (2)
C1–C2	1.527	1.528
C2–C3	1.561	1.562
C3–C4	1.557	1.559
C4–C5	1.572	1.575
C11–C12	1.513	1.518
C12–C13	1.469	1.345
C13–C14	1.509	1.506
C15–C16	1.516	1.517
C16–C17	1.348	1.348
C1–O	1.377	1.378
C12–O	1.464	
C13–O	1.467	
C1–C2–C3	114.3	114.8
C2–C3–C4	116.2	116.3
C11–C12–C13	120.2	119.9
C12–C13–C14	122.5	125.2
C13–C14–C15	113.9	116.1
C14–C15–C16	113.0	111.1
C12–O–C13	60.2	

<sup>a</sup> The atom numbers are defined in Scheme 1.

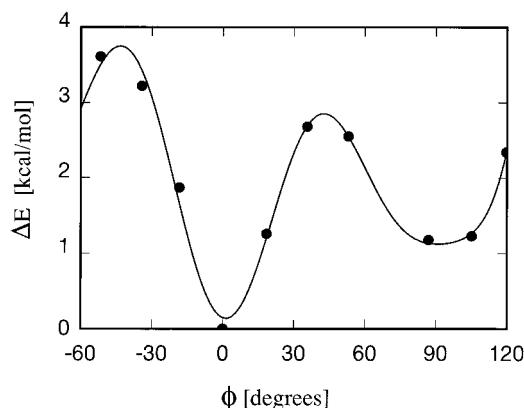


**Figure 2.** Potential energy of epothilone-A as a function of the C14–C15–C16–C17 torsion angle  $\phi$ . The zero of energy and angles correspond to the ground state geometry. The full line is a guide to the eye.

least for the gas phase molecules. Indeed, by interchanging the position of the H and of the OH attached to the C2' of paclitaxel (producing an isomer that displays lower anticancer activity than the previous one, see ref 5), a stronger intramolecular hydrogen bond is formed, lowering the energy by a small, but not negligible, amount (~2 kcal/mol). The simplicity of this transformation, together with the size and complexity of these molecules, suggests that a multitude of isomers can be found with an energy very close to (and often lower than) that of the forms with the highest anticancer activity.

A large stress in the carbon backbone is apparent also in epothilone-A, for which distortions in angles and distances are as important as those in the taxane ring of the paclitaxel family and probably due to the uneven distribution of oxygen in the main ring and in several side groups. Our computation has been able to show that either rotating or removing the residue at the C15 position has little effect on the structure of the central ring. We have first carried out tail rotations around the C15–C16 single bond and found only a very limited energy increase of less than 4 kcal/mol (see Figure 2; each configuration has been relaxed by a short MD annealing at fixed value of the  $\phi$  angle) accompanied by a minor stretching of the C15–C16 interatomic distance (see Figure 3).

In addition to tail rotations, we have modified epothilone-A in order to obtain by epothilone-B(2) (an analogue intensively

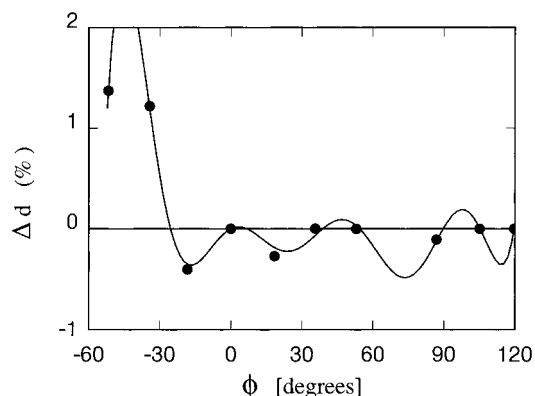


**Figure 3.** Variation of the C15–C16 bond length (in percent) upon rotation of the epothilone-A tail. The angle  $\phi$  is defined as in Figure 2. The full line is a guide to the eye.

**TABLE 3: Selected Interatomic Distances ( $\text{\AA}$ ) and Angles (deg) in (+)-Discodermolide and in One of Its Analogues Obtained by Cutting the Carbon Chain at C19<sup>a</sup>**

atoms	discodermolide	analogue
C5–C6	1.528	1.529
C6–C7	1.534	1.534
C7–C8	1.509	1.509
C8–C9	1.341	1.341
C9–C10	1.514	1.515
C10–C11	1.546	1.545
C11–C12	1.555	1.557
C12–C13	1.508	1.508
C17–C18	1.541	1.533
C18–C19	1.545	1.533
C19–O	1.481	
C5–C6–C7	113.9	114.5
C6–C7–C8	112.2	112.0
C7–C8–C9	128.2	128.0
C8–C9–C10	127.4	127.5
C9–C10–C11	111.6	111.1
C10–C11–C12	114.8	114.4
C12–C13–C14	129.1	129.5
C17–C18–C19	114.0	114.9
C18–C19–C20	116.9	

<sup>a</sup> The atom numbers are defined in Scheme 1.

investigated for its high activity<sup>15</sup>) by removing the epoxy oxygen and replacing the residue R by a methyl group. Careful relaxation of this molecule has shown that these chemical transformations change the epothilone structure only locally.<sup>13</sup> Beyond the nearest neighbors, the only noticeable effect is a slight enhancement of the deviation of angles and distances from the ideal ones, indicating increased stress in the structure.<sup>14</sup>

Despite its chain structure, a large stress in the bonds and bond angles is also present in discodermolide (see Table 3). As for epothilone, the substantial presence of oxygen in the chain and the irregular alternation of single and double bonds explain this large deformations in the structure. To investigate the interaction of the major chain with the tail, we have rotated the latter around the C18–C19 bond, performing a short molecular dynamics relaxation for each tail orientation. The energy required for the rotation is again relatively low (less than 8 kcal/mol), while the geometry of either the C1–C18 chain or of the tail changes little (nearest neighbor distances change by less than 0.02  $\text{\AA}$ ). Even the complete removal of the tail at the C18 position (saturated by an additional H atom) does not affect the structure of the main molecular body in a noticeable way.

#### 4. Charge Distribution and Electronic Structure

To identify the electrostatic “signature” of these molecules, the dipole moment of the ground-state structures are given in

**TABLE 4: Dipole Moment, of Taxol, Taxotere, Baccatin III, Epothilone-A, and Discodermolide<sup>a</sup>**

taxol	X	Y	Z
C2	−5.315	−3.468	−0.7467
C9	−3.104	−0.972	−0.551
C12	−6.609	−0.079	−0.433
dipole	−2.87	−4.27	−2.88
taxotere	X	Y	Z
C2	16.598	3.636	−3.698
C9	19.832	4.337	−4.135
C12	18.503	4.951	−0.821
dipole	−5.12	0.23	3.23
baccatin-III	X	Y	Z
C2	−4.467	−3.896	−0.224
C9	−3.140	−0.959	−0.551
C12	−6.664	−0.097	−0.469
dipole	−4.52	−3.90	−0.58
epothilone-A	X	Y	Z
C1	0.271	−0.687	1.173
C7	−4.003	3.791	1.265
C12	−1.666	1.377	−3.127
dipole	2.45	1.50	1.87
discodermolide	X	Y	Z
C1	6.796	3.904	0.613
C11	8.701	10.798	−1.789
C18	11.607	5.402	−5.288
dipole	−0.66	2.16	−2.80

<sup>a</sup> The coordinates of three atoms (in  $\text{\AA}$ ) define the relative orientation of the dipole (in debye) with respect to the molecule. Atom numbers are defined in Scheme 1.

Table 4 together with the coordinates of three atoms defining the molecular orientation. Baccatin, paclitaxel, and taxotere have nearly identical dipole moments ( $\sim 6$  D), suggesting that this is located exclusively on the taxane ring. The moment lies approximately in the taxane plane, pointing toward the tail. Epothilone-A has a somewhat smaller but still sizable (3.4 D) dipole moment, whose orientation is analogous to the one in the paclitaxel family: the dipole lies in the lactone plane, pointing toward the tail. In this case as well, the dipole resides mainly on the central body atoms, although the moment associated with the tail is not negligible: upon substituting the residue at the C15 carbon by a single H, the modulus of the dipole moment remains almost unchanged, but its direction rotates by  $\sim 20^\circ$  while remaining in the lactone plane. The dipolar signature of discodermolide is also similar to those of the previous molecules: the total dipole (3.6 D) is closer to that of epothilone than to those of the taxoids, pointing once again approximately toward the tail. As in epothilone, the dipole associated to the tail is small but not negligible: removing the residue at C18 increases the total moment to 5 D, while rotating its direction by  $\sim 15^\circ$ .

The global description of the molecular electrostatics provided by the dipole moment is supplemented by the computation of the atomic charges reproducing the electrostatic potential around the molecules (the so-called “ESP” charges, see ref 16 for a recent discussion). The obtained charges represent an essential ingredient for the atomistic simulation of these molecules and are provided as Supporting Information.

As an additional way to characterize the electron distribution, we compute the atomic Mulliken charges, obtained by projecting the Kohn–Sham eigenstates onto a minimal basis of atomic pseudo wave functions. The projection has a satisfactory degree



of completeness (less than 1.4% of the charge is unassigned for each molecule). The derivatives of the Mulliken population with respect to the molecular charge are connected to the Fukui characterization of the molecular reactivity.<sup>17</sup> We evaluated those derivatives by performing a series of electronic structure computations at fixed geometry, with different fractional populations in the molecular orbitals corresponding to the highest occupied and lowest unoccupied Kohn–Sham levels of the neutral ground state. Since negative ions are not stable in our DFT scheme, we use only configurations with zero or positive net charge in the evaluation of both the left and right derivatives with respect to the total charge density.<sup>18</sup> The results show that, as expected, all these molecules display rather low reactivity, distributed among many atoms, without a well-defined active center.

In the taxoids, the C8–C12 segment is the preferred region for electrophilic attack, and the AR1 phenyl is the most reactive group for nucleophilic reagents. The tails of both paclitaxel and taxotere do not appear to be particularly reactive. In epothilone-A, reactions with nucleophilic species are possible in the segment of the lactone ring extending from C5 to C7, and including the neighboring oxygens. Electrophilic (and radical) attack is possible at the tail. Discodermolide presents a region favorable to nucleophilic reagents in the long chain (C9, C10, and C27), while the tail is reactive with respect to electrophilic and radical attack. This result shows that these molecules are similar, all having an extended nucleophilic reaction region at the center of the main molecular body. The similarity is even stronger for epothilone-A and discodermolide, as both have the preferred site for electrophilic reactions in the tail. Unfortunately, despite these similarities there is no simple way to derive the pharmacophore mechanism of these drugs. Indeed, attempted rigid rotations and translations of the taxoids, epothilone, and discodermolide molecules were not adequate to obtain a sufficient overlap of their respective reaction centers.

Despite some indirect indications,<sup>19</sup> it is not clear whether chemical transformations play a role in the interaction of any of these molecules with tubulin. These could be mediated mainly by nonbonded interactions, in which case the distribution of reaction centers would play a limited role in the pharmacophore activity, giving only indications on the spatial affinity for certain substrate groups of these molecules. Steric effects and the presence of a sizable dipole could then be the important factors.

## 5. Vibrational Properties

The structural and electrostatic properties described in the previous section are necessary but not sufficient information to build an atomistic model of these compounds. To this aim, dynamical properties are required in order to define the value of stretching, bending and torsional force constants.

For this reason, we computed the vibrational modes of baccatin-3, taxol, epothilone-A, and discodermolide. The results are available as Supporting Information.

The vibrational properties of all these molecule are similar and display a clear correlation with the structural and bonding properties. As expected, the highest frequencies ( $\sim 3500\text{ cm}^{-1}$ ) belong to the OH and NH stretching modes, which are infrared active and can easily be detected in experiments. The formation of intramolecular hydrogen bonds is revealed by a decrease of the corresponding OH frequency by  $\sim 80\text{ cm}^{-1}$ , the shift being larger for the shortest and most linear O–H–O bonds. All the other stretching modes involving hydrogen populate a band extending from 2950 to 3150  $\text{cm}^{-1}$ . A gap separate this band from an isolated peak in the vibrational density of states located

at 1680–1750  $\text{cm}^{-1}$ , containing all the C=O stretching modes. Below  $\sim 1600\text{ cm}^{-1}$  all these molecules present a rather unstructured vibrational density of states, extending down to the lowest frequencies. Interestingly, although not unexpectedly, there is a clear correlation between the frequency of the eigenmodes and the strain of the interatomic bonds supporting them: within each vibrational band (i.e., stretching, bending and torsion of each chemical bond type) higher frequencies are computed for modes localized on highly strained groups of atoms.

Since these last computations have been motivated by providing data for empirical modeling, we comment in this section on preliminary tests of standard force fields for these molecule. We used the TRIPOS 5.2 model with the parameters reported in ref 20 to relax the structure of the simplest among these molecules, i.e., baccatin. The results show that, although the experimental structure is still clearly recognizable in the relaxed geometry, at the quantitative level there are also significant deviations,<sup>21</sup> especially in the degrees of freedom (like torsional angles) associated with soft restoring forces. Moreover, the vibrational frequencies are overestimated with respect to the DFT results (by as much as 50%). In the absence of detailed experimental results for many of these quantities, we expect that refining the interatomic force constants in order to reproduce the DFT data could provide a significant improvement of the force field parametrization. Work is in progress along this line.

## 6. Conclusions

Although unknown in its details, the mechanism for the anticancer activity of paclitaxel, taxotere, epothilone-A, and discodermolide appears to be very similar, being related to the alteration of the polymerization equilibrium of tubulin. The similarity in the activity is accompanied by a similarity in structure: all these compounds are small/medium size organic molecules, characterized by a central body and a protruding tail. The computations show that the similarities extend much deeper than a generic resemblance in shape and involve also their electronic structures. In our calculations, the central part of all these molecules appears to be rigid to changes in structure, orientation, and isomerization of its tail and is characterized by a rather large dipole that has similar orientation with respect to the molecular frame. The investigation of a few isomers and analogues shows that every modification known to increase the pharmacological activity of the drugs also enhances these peculiar features.

These properties could correlate with the experimental observation that all the active species share the same docking site to tubulin, as inferred from the fact that their binding to tubulin is competitive and mutually exclusive.<sup>1b</sup> We might speculate that the central molecular body has to dock to a well-defined and rather selective binding site, with the dipole providing a medium-/long-range guidance for the binding. On the other hand, the tail is both rigid and connected to the central body by a flexible link, suggesting that this part of the molecule could be used for an adaptive link to a neighboring docking site, on either the same or a different tubulin dimer.

To conclude, although we have been unable to identify possible candidates for binding sites in the molecules based on the electronic properties and structure of these molecules, our study supplies an extended set of structural and energy data (available as Supporting Information). This material will contribute significantly in the development of simplified yet reliable molecular mechanics models for these drugs which,

combined with existing protein force field, can be used in an atomistic investigation of the drug–tubulin interaction. The interest in such an approach is greatly enhanced by the recent publication of the tubulin structure.<sup>2</sup>

**Acknowledgment.** We thank P. Procacci for useful discussions and R. O. Jones for a careful re-reading of the manuscripts. We are grateful to the computer center of the Commissariat à l'Énergie Atomique in Grenoble for a generous allocation of computer time.

**Supporting Information Available:** The optimized structure and electrostatic atomic charges of paclitaxel, taxotere, baccatin-II, epothilone-A, and discodermolide. The structure of isomers of paclitaxel and taxotere is also provided. This material is available free of charge via the Internet at <http://pubs.acs.org>.

## References and Notes

- (1) (a) Horwitz, S. B. *Trends Pharm. Sci.* **1992**, *13*, 134–136. (b) Cowden, C. J.; Paterson, I. *Nature* **1997**, *387*, 238–239.
- (2) Nogales, E.; Wolf, S. G.; Downing, K. H. *Nature* **1998**, *391*, 199–202. Löwe, J.; Amos, L. A. *Nature* **1998**, *391*, 203–206.
- (3) Paclitaxel: Mastropaolo, D., et al. *Proc. Natl. Acad. Sci. U.S.A.* **1995**, *92*, 6920. Taxotere: Gueritt-Voegelein, F., et al. *Acta Crystallogr., C (Cr. Str. Comm.)* **1990**, *46*, 781. Baccatin III: we started from the paclitaxel structure after removing the residue at C13. Epothilone-A: Höfle, G., et al., *Angew. Chem., Int. Ed. Engl.* **1996**, *35*, 1567. Discodermolide: Gunasekera, S. P.; Gunasekera, M.; Longley, R. E. *J. Org. Chem.* **1990**, *55*, 4912.
- (4) Gueritt-Voegelein, F., et al. *J. Med. Chem.* **1991**, *34*, 992.
- (5) Swindell, C. S., et al. *J. Med. Chem.* **1991**, *34*, 1176.
- (6) Car, R.; Parrinello, M. *Phys. Rev. Lett.* **1985**, *55*, 2471. Computations are performed using the CPMD program version 3.0, J. Hutter et al., MPI für Festkörperforschung and IBM Research, 1990–1997.
- (7) Jones, R. O.; Gunnarsson, O. *Rev. Mod. Phys.* **1989**, *61*, 689. Parr, R. G.; Yang, W. *Density Functional Theory of Atoms and Molecules*; Oxford University Press: Oxford, UK, 1989.
- (8) We use the interpolation of: Perdew, J. P.; Zunger, A. *Phys. Rev. B* **1981**, *23*, 5048, for the electron gas correlation energy. We use the gradient correction of Becke for exchange (Becke, A. D. *J. Chem. Phys.* **1986**, *84*, 4524), and of Perdew (Perdew, J. P. *Phys. Rev. B* **1986**, *33*, 8822) for correlation.
- (9) Troullier, N.; Martins, J. L. *Phys. Rev. B* **1991**, *43*, 1993.
- (10) The plane wave expansion for the Kohn–Sham orbitals implies an artificial periodicity in real space. For each molecule we consider a simulation cell whose dimension is such that the interaction of periodic replicas is negligible.
- (11) In most cases, the relaxed interatomic distances differ from the experimental ones by less than 0.05 Å, while bending angles change by less than 0.5 Å. Torsional angles display larger deviations, possibly reflecting their dependence on the crystal versus gas-phase environment.
- (12) The three intramolecular hydrogen bonds in paclitaxel join the OH group at C2' to oxygen at C1'; OH at C7 to O at C9; OH at C1 to the oxygen closest to the Ar1 group. In all these bonds the O–O and O–H distances are shorter than 2.95 Å.
- (13) The C12–C13 distance changes from 1.34 Å in epothilone-A to 1.47 Å in epothilone-B(2). However, both the C11–C12 and C13–C14 distances change by less than 0.005 Å.
- (14) For instance, the sp<sup>2</sup> C12–C13–C14 bending angle changes from 122.6° in A to 125.2° in B(2), respectively, while the corresponding values for the sp<sup>3</sup> angle C10–C11–C12 are 108.5° and 106.1° (B(2)).
- (15) Nicolau, K. C., et al. *Nature* **1997**, *387*, 268.
- (16) Hawkins, G. D.; Cramer, C. J.; Truhlar, D. G. *J. Chim. Phys. (Paris)* **1997**, *94*, 1448–1481.
- (17) Fukui, K. *Science* **1982**, *217*, 747; the extension to derivatives of the Mulliken charges with respect to occupation is described by: Yang, W.; Mortier, W. J. *J. Am. Chem. Soc.* **1986**, *108*, 5708.
- (18) The right ( $F_A^+$ ), left ( $F_A^-$ ) and central derivatives of the Mulliken population on atom A is computed as:  $F_A^+ = [Q_A(f_H - \delta, f_L + \delta) - Q_A(f_H - \delta, f_L)]/\delta$ ,  $F_A^- = [Q_A(f_H, f_L) - Q_A(f_H - \delta, f_L)]/\delta$ , and  $F^0 = [Q_A(f_H - \delta, f_L + \delta) - Q_A(f_H, f_L)]/\delta$ , where  $Q_A(f_H, f_L)$  is the Mulliken charge on atom A when the population of the highest occupied and lowest unoccupied molecular orbital is  $f_H$  and  $f_L$ , respectively.
- (19) Mellado, W., et al. *Biochem. Biophys. Res. Commun.* **1984**, *124*, 329.
- (20) Clark, M., et al. *J. Comput. Chem.* **1989**, *10*, 982.
- (21) In the case of baccatin-III, the average deviation between the DFT and the force field results amount to 0.02 Å and 1° for interatomic distances and angles, respectively. The average has been computed for the distances and angles listed in Table 1. Torsion angles may differ by as much as 10°. Not surprisingly, deviations are more important for unusual bonding configurations, like those in the C4–C5–O–C20 ring.